

(control) antibodies using Mep HyperCel (Pall Life Sciences, Cerg, FGrance) and DEAE cellulose chromatographies. HMGB1 neutralizing activity was confirmed by determining its ability to attenuate HMGB1 bioactivity on cultured macrophages as previously described.<sup>1</sup>

## **HMGB1**

Full-length recombinant HMGB1 was purchased from HMGBiotech (Milano, Italy); it was purified as previously described and endotoxins were removed by passage through Detoxy-Gel columns (Pierce Chemical Co).<sup>4,5</sup> HMGB1 was rigorously tested to be LPS-free.<sup>6</sup>

## **Plasma Cholesterol and Triglycerides**

Plasma LDL- and HDL-cholesterol were determined enzymatically using a Cobas Mira Plus Autoanalyzer and a HDL and LDL/VLDL cholesterol quantification kit (BioVision, Mountain View, CA). Plasma triglycerides were determined using a triglyceride quantification kit (BioVision, Mountain View, CA).

## **Quantification of Atherosclerotic Lesions**

The heart and proximal aorta were dissected from mice, embedded in OCT compound (Tissue-teck) and frozen at -80°C. Frozen sections (6µm) were cut from the aortic sinus, from where the valves or valve cusps first become visible to where the left and right coronary arteries branch off, a distance of approximately 250µm.<sup>7</sup> A total of 4 sections taken from identical aortic sinus locations in each mouse at 60µm intervals were stained with Oil Red O to delineate lipid deposits and counter stained with haematoxylin.<sup>8</sup> The aortic sinus was evaluated because this region of the aorta is particularly susceptible to the development of atherosclerotic lesions in mice fed a high fat diet.<sup>7</sup> Sections were examined using light microscopy and the cross-sectional area of lipid depositions quantified using image analysis software (Optimus 6.2 VideoPro-32). For each mouse, the

lesion size was measured in 4 cross-sections and lesion size per cross-section averaged to provide the mean lesion size per mouse.

### **Immunohistochemistry**

Twenty seven 6 $\mu$ m cryo-sections from similar parts of the aortic sinus of ApoE<sup>-/-</sup> mice treated with control or anti-HMGB1 neutralizing antibody were used for immunohistochemistry to assess macrophage accumulation (CD68), CD4<sup>+</sup> T-lymphocytes, dendritic cells (CD11c), vascular smooth muscle cells (alpha SM actin) and endothelial cells (CD31), VCAM-1, MCP-1, CD83, HMGB1 and PCNA. Briefly, sections were fixed in cold (-20°C) acetone for 20 min. The sections were then incubated in 3% hydrogen peroxide in PBS, 10% normal serum and biotin/avidin blocking reagents (Vector Laboratories). Then the sections were incubated (1hr) with primary antibodies in serum, rat anti-mouse CD68 (1-100; Serotec: cat#MCA1957), Armenian hamster anti-mouse CD11b (1-50; eBioscience: cat#14-0114), rat anti-mouse CD4 (1-20; BD Pharmingen: Cat#550280), rabbit anti-alpha smooth muscle actin (1-100; Abcam: #ab5694), rat anti-mouse CD31 (1-100, BD Pharmingen: cat# 550274), rat anti-mouse VCAM-1 (1-50; BD Pharmingen: cat#550547), rabbit anti rat MCP-1 (1-50; Abcam: cat#ab7202), rat anti-mouse CD83 (1-50; eBioscience: cat#14-0831), rabbit anti-HMGB1 antibody (0.125 $\mu$ g/ml; BD Pharmingen: cat#556528) and rabbit anti-human PCNA (1-50; Abcam: cat#ab2426). Subsequently the sections were washed and incubated with the appropriate secondary antibody [biotinylated mouse anti-rat (1-200; BD Pharmingen: cat#550325), biotinylated mouse anti-Armenian hamster (1-200; eBioscience: cat#13-4113-85) or biotinylated anti-rabbit (1-200; Vector Labs: cat#BA-1000)] for 40 minutes, followed by incubation with streptavidin horseradish peroxidase complex (Vector Laboratories). Antigens were visualized using 3,3-diaminobenzidine.<sup>9</sup> Sections were counterstained with hematoxylin. Expression of antigens was quantified either by cell counting or measuring stained areas using Optimus 6.2 VideoPro-32 and results expressed either as stained cross-sectional

area (CD68), cells per unit area (CD4, PCNA) or percent of total plaque area (CD31, alpha-SM actin, CD11c, CD83, VCAM-1, MCP-1).<sup>10</sup>

### **mAbs and Flow Cytometry**

The following antibodies were used: anti-CD4-pacific blue (BD Pharmingen), anti-CD8-PerCP (BD Pharmingen), anti-TCR $\beta$ -APC (Pharmingen), anti-NK1.1-PE Cy7 (Pharmingen), anti-CD25-APC Cy7 (Pharmingen), Foxp3-PE (BD Pharmingen), anti-CD11c-PE (eBioScience), anti-F4/80-Alexafluor (647) eBioScience), anti-CD11b-PerCP-Cy5.5 (eBioScience) and anti-Gr1 (Ly6G and Ly6C)-AlexaFluor-488 (eBioScience).<sup>11</sup>

Spleens and lymph nodes were gently dissociated between the frosted ends of glass slides to obtain single cell suspensions which were passed through a 70 $\mu$ M nylon strainer. Single cell suspensions were pre-incubated with anti-FcR $\gamma$  (2.4G2) to prevent non-specific staining followed by incubation with fluorochrome-conjugated primary antibodies for 30 minutes at 4°C. For Foxp3 staining the cells were permeabilized using the BD Pharmingen Mouse Foxp3 buffer set according to the manufacture's directions. For analyses of monocytes and dendritic cells in blood and lymph nodes the following antibodies were used: NK1.1-PE, CD22-PE, CD90-PE, CD49b-PE, Ly-6G-PE, CD11b-APC-Cy7, Ly-6C-pacific blue, CD11c-APC and BrdU-PerCP (all from BD Pharmingen), I-A<sup>b</sup>-PE-Cy7 (BioLegend) and CD115-Alexa-488 (eBiosciences). Monocytes in blood were identified as CD11b<sup>hi</sup>CD90<sup>lo</sup>CD22<sup>lo</sup>CD49b<sup>lo</sup>NK1.1<sup>lo</sup>Ly-6G<sup>lo</sup> and monocyte-derived dendritic cells as CD11c<sup>hi</sup>CD11b<sup>hi</sup>CD90<sup>lo</sup>CD22<sup>lo</sup>CD49b<sup>lo</sup>NK1.1<sup>lo</sup>Ly-6G<sup>lo</sup>.<sup>12</sup> Sample data was acquired using a BD FACS Canto II (BD Biosciences).

### **HMGB1 Elisa**

HMGB1 in plasma was measured using an ELISA HMGB1 detection kit (Apotech Corp, Enzo Life Sciences GMBH, Germany) according to the manufacture's instructions. The sensitivity of the assay is approximately 1ng/ml.

## **Macrophage Chemotaxis in Vitro and in Vivo**

Macrophage chemotaxis in vitro was measured using fibronectin-coated-8 $\mu$ m porous transwells (BD Biosciences). Briefly, RAW264.7 mouse macrophages (200,000) were cultured in DMEM containing 1% fetal calf serum prior to being loaded onto the inserts which were placed in 24-well plates containing DMEM in the presence or absence of 4 $\mu$ g/ml HMGB1 and incubated at 37°C for 15 hours. Non-migrated cells in the top chamber were removed using cotton swabs before fixing the migrated cells in methanol-glacial acetic acid (3:1) and staining with crystal violet. Chemotaxis was quantified by counting the number of migrated in five random high-power microscopy fields per well.<sup>13</sup> To determine whether HMGB1 induced macrophage chemotaxis in vivo mice were injected i.p. with 1ml of vehicle (0.9% NaCl) or HMGB1 (20 $\mu$ g/ml in 0.9% NaCl). After 5 hours the mice were sacrificed and the cellular contents of their intraperitoneal cavities were collected by sequential lavages in PBS. After centrifugation, red blood cells were lysed with ammonium chloride-potassium carbonate-EDTA buffer (0.15M NH<sub>4</sub>Cl, 1mM KHCO<sub>3</sub> and 0.1mM Na<sub>2</sub>EDTA in PBS) and total cell numbers determined. Then the cells were pre-incubated with anti-FcR $\gamma$  (2.4G2) to prevent non-specific staining followed by incubation with fluorochrome-conjugated primary antibodies-anti-F4/80, anti-CD11b, anti-CD11c and anti-Gr-1 (see mAbs and Flow Cytometry) for 30 minutes at 4°C. Sample data was acquired using a BD FACS Canto II (BD Biosciences).

## **Analysis of Gene Expression**

Total RNA was extracted from tissues as previously described<sup>14</sup> and resuspended in sterile water; any contaminating DNA was removed by incubating the RNA extracts with 2 U DNase (Stratagene), for 15 minutes at 37°C. Then 2  $\mu$ L of 2 mol/L sodium acetate followed by an equal volume of isopropanol was added and the precipitated RNA was sedimented by centrifugation. The RNA pellet was washed by resuspension in 70% aqueous ethanol followed by centrifugation, and then air dried for 30 minutes. This purified RNA was dissolved in sterile water and quantitated by spectrophotometry at 260 nm. The

extracted total RNA was reverse transcribed using TaqMan methodology (Applied Biosystems) as described by the manufacturer. Then 40ng of cDNA was used for real-time PCR to determine the expression of each gene using Applied Biosystems SYBR Green PCR Mix and the ABI Prism 7500 system. Each amplification was performed in duplicate and included internal controls for CD68 (macrophages) to take into account any alterations in lesion size. Relative amounts of each mRNA for each of the genes in lesions from control and anti-HMGB1 treated ApoE<sup>-/-</sup> mice were calculated using comparative C<sub>T</sub> values.<sup>4</sup> The sequences of oligonucleotides used were, TIM-1: sense, 5'-AGTGACCTTTTCATTGCAAGTTAAAC-3' and antisense, 5'-GCTGTGG GCCTTG TAGTTGTG-3'; for TIM-3: sense, 5'-CAGCTTCTCCAAGAACCCTAACC-3' and antisense, 5'-TTATTATGGAGGGTCACCAGTGTCT-3'; for IL-6: sense, 5'-GAAATGAT GGATGCTACCAAAGT-3' and antisense, 5'-CCAGAAGACCAGAGGAAATTTTCA-3'; for TNF- $\alpha$ : sense, 5'-CTATGGCCCAGACCCTCACA-3' and antisense, 5'-TCCTCCACTTG GTGGTTTGC-3'; for IFN- $\alpha$ : 5'-TCCTCAGACTCATAACCTCAGGAA-3' and antisense, 5'-GGGAGAGTCTCCTCATTTGTACCA-3'; for IL-1 $\beta$ : sense, 5'-CCACCTCAATGGACAGAA TATCAA-3' and antisense, 5'-GTCGTTGCTTGGTTCTCCTTGT-3'; for 18s: sense, 5'-CGGCTACCACATCCAAGGAAGGCA-3' and antisense, 5'-GCTGGAATTACCGCGGCTGCTGGC-3' ; for CD68: sense, 5'-TGACCTGCTCTCTCTAAGGCTACA-3 and antisense, 5'-TGGTCACGGTTGCAAGAGAA-3.

### **Statistical Analyses**

Statistical analyses were performed using Student's t-test when data followed a normal distribution or Mann-Whitney U test when data did not follow a normal distribution, using the software GraphPad Prism v4.01. P < 0.05 was considered statistically significant.

## References for Supplemental Materials and Methods

1. Liu K, Mori S, Takahashi HK, Tomono Y, Wake H, Kanke T, Sato Y, Hiraga N, Adachi N, Yoshino T, Nishibori M. Anti-high mobility group box 1 monoclonal antibody ameliorates brain infarction induced by transient ischemia in rats. *FASEB J.* 2007; 21: 3904-3916.
2. Mittler RS, Bailey TS, Klussman K, Trailsmith MD, Hoffmann MK. Anti-4-1BB monoclonal antibodies abrogate T cell-dependent humoral immune responses in vivo through the induction of helper T cell anergy. *J Exp Med.* 1999; 190: 1535-1540.
3. Vieira P, Rajewsky K. The half-lives of serum immunoglobulins in adult mice. *Eur J Immunol.* 1988; 18: 313-316.
4. Palumbo R, Sampaolesi M, De Marchis F, Tonlorenzi R, Colombetti S, Mondino A, Cossu G, Bianchi ME. Extracellular HMGB1, a signal of tissue damage, induces mesoangioblast migration and proliferation. *J Cell Biol.* 2004; 164: 441-449.
5. Muller S, Bianchi ME, Knapp S. Thermodynamics of HMGB1 interaction with duplex DNA. *Biochemistry.* 2001; 40: 10254-10261.
6. Penzo M, Molteni R, Suda T, Samaniego S, Raucci A, Habel DM, Miller F, Jiang H, Li J, Pardi R, Palumbo R, Olivetto E, Kew RR, Bianchi ME, Marcu KB. Inhibitor of NF- $\kappa$ B kinases  $\alpha$  and  $\beta$  are both essential for high mobility group Box 1-mediated chemotaxis. *J Immunol.* 2010; 184: 4497-4509.
7. Paigen B, Morrow A, Holmes PA, Mitchell D, Williams RA. Quantitative assessment of atherosclerotic lesions in mice. *Atherosclerosis* 1987; 68: 231-240.
8. Lewis P, Stefanovic N, Pete J, Calkin AC, Giunti S, Thallas-Bonke V, Jandeleit-Dahm KA, Allen TJ, Kola I, Cooper ME, de Haan JB. Lack of the antioxidant enzyme glutathione peroxidase-1 accelerates atherosclerosis in diabetic apolipoprotein E-deficient mice. *Circulation.* 2007; 115: 2178-2187.

9. To K, Agrotis A, Besra G, Bobik A, Toh BH. NKT cell subsets mediate differential proatherogenic effects in ApoE<sup>-/-</sup> mice. *Arterioscler Thromb Vasc Biol.* 2009; 29: 671-677.
10. Raj T, Kanellakis P, Pomilio G, Jennings G, Bobik A, Agrotis A. Inhibition of fibroblast growth factor receptor signaling attenuates atherosclerosis in Apolipoprotein E-deficient mice. *Arterioscler Thromb Vasc Biol.* 2006; 26: 1845-51.
11. Daley JM, Thomay AA, Connolly MD, Reichner JS, Albina JE. Use of Ly6G-specific monoclonal antibody to deplete neutrophils in mice. *J Leukocyte Biol.* 2008; 83: 64-70.
12. Swirski FK, Libby P, Aikawa E, Alcaide P, Luscinskas FW, Weissleder R, Pittet MJ. Ly-6C<sup>hi</sup> monocytes dominate hypercholesterolemia-associated monocytosis and give rise to macrophages in atheroma. *J Clin Invest.* 2007; 117: 195-205.
13. Chiou W-F, Shum A Y-C, Peng C-H, Chen C-F, Chou C-J. Piperlactam S suppresses macrophage migration by impeding F-actin polymerization and filopodia extension. *Eur J Pharmacol.* 2003; 458: 217-225.
14. Ward MR, Agrotis A, Kanellakis P; Dilley R, Jennings G, Bobik A. Inhibition of Protein Tyrosine Kinases Attenuates Increases in Expression of Transforming Growth Factor- $\beta$  Isoforms and Their Receptors Following Arterial Injury. *Arterioscler Thromb and Vasc Biol.* 1997;17:2461-2470.



## Legends for Supplementary Tables and Figures

**Table I:** Plasma Lipid Levels in ApoE<sup>-/-</sup> mice treated with control or anti-HMGB1 antibody (Ab) and fed a high fat diet for 8 weeks. Results are means  $\pm$  SEM.

**Table II.** Monocyte subtypes and dendritic cells in blood (cells/ml) and lymph nodes (cell numbers) of ApoE<sup>-/-</sup> mice treated with control or anti-HMGB1 antibody (Ab) and injected with bromodeoxyuridine (1mg, i.p.) for 3 consecutive days before culling. Results are means  $\pm$  SEM of 4 mice in each group.

**Figure I.** Immunohistochemistry of aortic sinus atherosclerotic lesions from control (left) and anti-HMGB1 neutralizing antibody (right) treated ApoE<sup>-/-</sup> mice fed a high fat diet. Cross sections were stained with anti-alpha-SM actin antibody to detect smooth muscle cells associated with lesions (top), anti-CD31 antibody to detect endothelial cells associated with lesions (middle) and anti-proliferating nuclear antigen (PCNA) antibody to detect cell proliferation (bottom). Bar graphs represent differences between the two groups. Red: control and blue: anti-HMGB1 antibody treatment. \*P < 0.05 from control. Size bars on photomicrographs represent 100 $\mu$ m.

**Figure II.** Lymphocyte populations (CD4<sup>+</sup> T cells, CD19<sup>+</sup> B cells, NK1.1<sup>+</sup> NK cells, NK1.1<sup>+</sup>TCR<sup>+</sup> NKT cells and CD4<sup>+</sup>Foxp3<sup>+</sup> regulatory T cells [Tregs]) in blood, spleen and para-aortic lymph nodes following treatment with control (open boxes) or anti-HMGB1 neutralising antibodies (shaded boxes). Bar graphs represent means  $\pm$  SEM of three mice in each group.

**Figure III.** Expression of proinflammatory mediators in atherosclerotic lesions following treatment with control (left) or anti-HMGB1 neutralizing antibodies (right). Top, photomicrographs of aortic sinus lesions stained with anti-VCAM-1 antibodies; middle:



aortic lesions stained with anti-MCP-1 antibodies and bottom real time PCR analyses of TNF- $\alpha$ , IFN- $\alpha$ , IL-6 and IL-1 $\beta$  expression in aortic atherosclerotic lesions. Bar graphs represent differences between the two groups. Red: control and blue: anti-HMGB1 antibody treatment. \*P < 0.05 from control. Size bars on photomicrographs represent 100 $\mu$ m

**Table I**

<b>Treatment</b>	<b>Total Cholesterol (mmol/l)</b>	<b>HDL-Cholesterol (mmol/l)</b>	<b>LDL-cholesterol (mmol/l)</b>	<b>Triglycerides (mmol/l)</b>
<b>Control Ab</b>	7.55 ± 0.33	1.27 ± 0.05	5.19 ± 0.22	2.46 ± 0.22
<b>HMGB1 Ab</b>	7.70 ± 0.38	1.30 ± 0.08	5.45 ± 0.29	2.14 ± 0.13

**Table II**

<b>MONOCYTE/DENDRITIC CELLS*</b>	<b>Control Ab</b>	<b>Anti-HMGB1 Ab</b>
<b>Blood</b>		
BrdU+CD11b <sup>hi</sup> Ly-6C <sup>hi</sup>	0.032 ± 0.017 x 10 <sup>6</sup>	0.044 ± 0.009 x 10 <sup>6</sup>
CD11b <sup>hi</sup> Ly-6C <sup>hi</sup>	0.103 ± 0.045 x 10 <sup>6</sup>	0.099 ± 0.024 x 10 <sup>6</sup>
CD11b <sup>hi</sup>	0.137 ± 0.056 x 10 <sup>6</sup>	0.130 ± 0.024 x 10 <sup>6</sup>
BrdU+CD11c <sup>hi</sup> CD11b <sup>hi</sup>	0.0348 ± 0.016 x 10 <sup>6</sup>	0.0394 ± 0.008 x 10 <sup>6</sup>
CD11c <sup>hi</sup> CD11b <sup>hi</sup>	0.082 ± 0.035 x 10 <sup>6</sup>	0.088 ± 0.025 x 10 <sup>6</sup>
CD11c <sup>hi</sup> CD11b <sup>hi</sup> I-A <sup>b(hi)</sup> CD115 <sup>hi</sup>	0.0097 ± 0.0048 x 10 <sup>6</sup>	0.0111 ± 0.0027 x 10 <sup>6</sup>
<b>Inguinal Lymph Nodes</b>		
CD11c <sup>hi</sup> CD11b <sup>hi</sup> I-A <sup>b(hi)</sup> CD115 <sup>hi</sup>	0.007 ± 0.003 x 10 <sup>6</sup>	0.008 ± 0.003 x 10 <sup>6</sup>
<b>Mediastinal Lymph Nodes</b>		
CD11c <sup>hi</sup> CD11b <sup>hi</sup> I-A <sup>b(hi)</sup> CD115 <sup>hi</sup>	0.0014 ± 0.004 x 10 <sup>6</sup>	0.0027 ± 0.0021 x 10 <sup>6</sup>

\* All cells are CD90<sup>lo</sup>CD49b<sup>o</sup>NK1.1<sup>lo</sup>Ly-6G<sup>lo</sup>CD22<sup>o</sup>

Figure 1

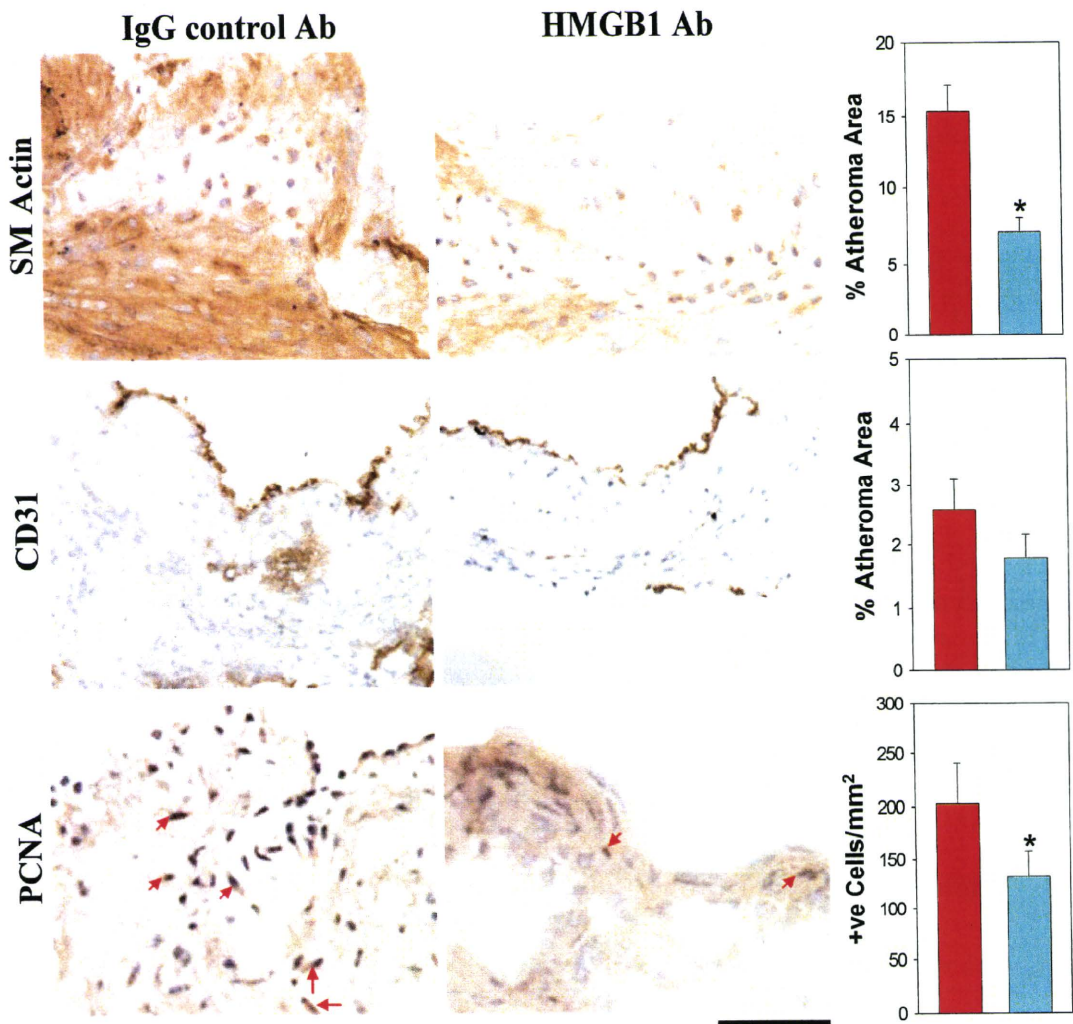
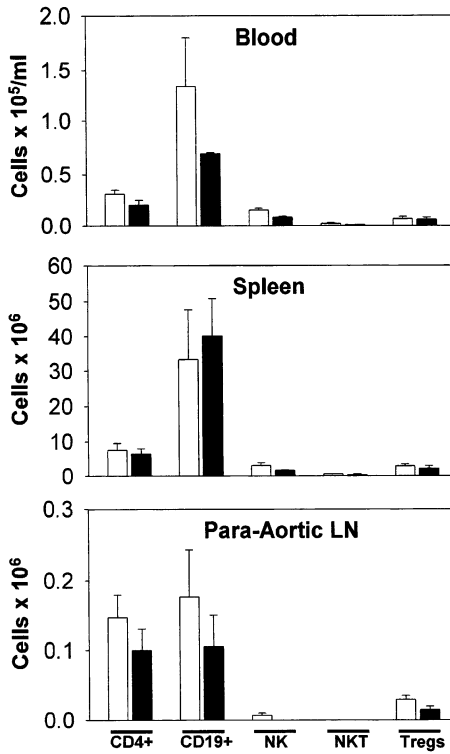
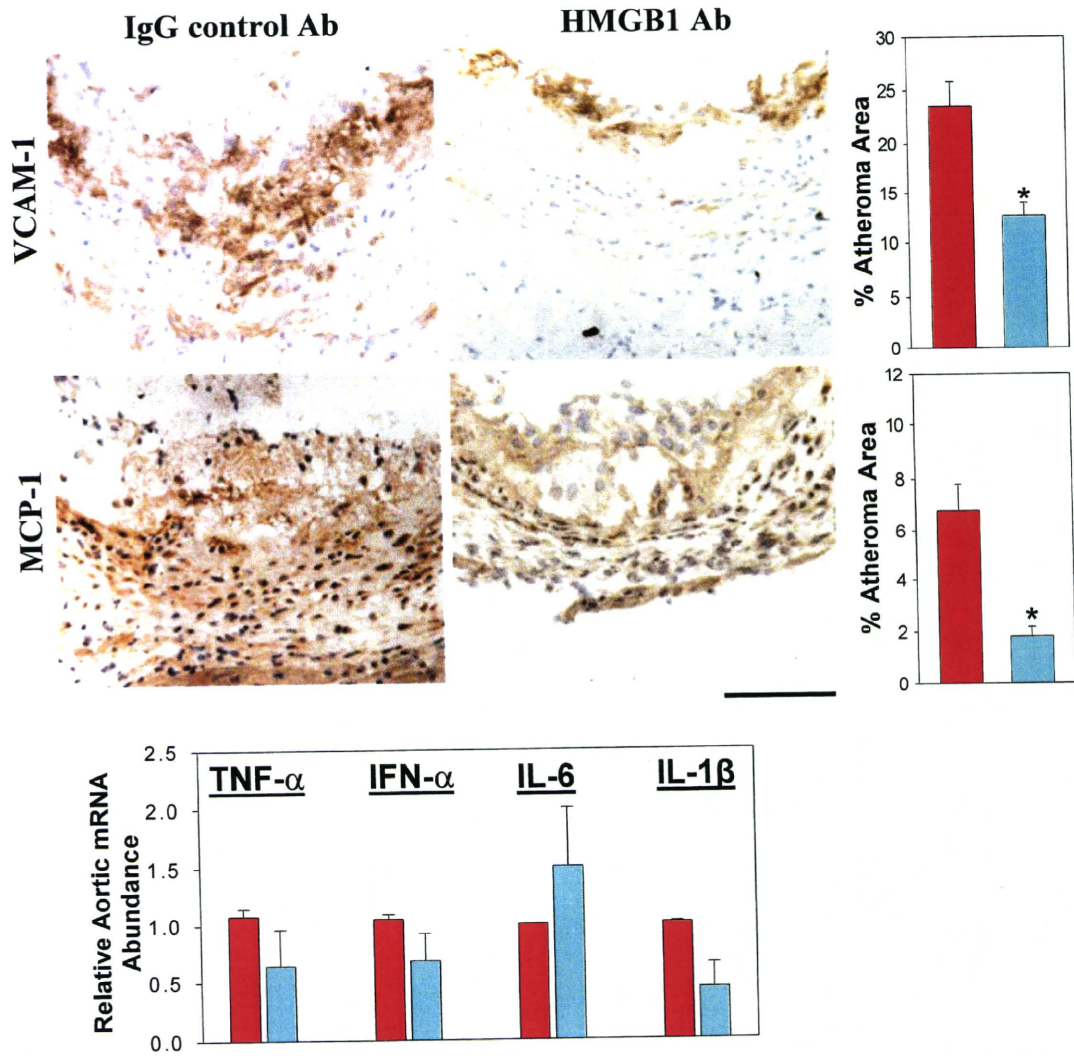


Figure II



**Figure III**



# Anti-high Mobility Group Box-1 Monoclonal Antibody Protects the Blood–Brain Barrier From Ischemia-Induced Disruption in Rats

Jiyong Zhang, PhD\*; Hideo K. Takahashi, MD, PhD\*; Keyue Liu, MD, PhD; Hidenori Wake, PhD; Rui Liu, PhD; Tomoko Maruo, MD; Isao Date, MD, PhD; Tadashi Yoshino, MD, PhD; Aiji Ohtsuka, MD, PhD; Shuji Mori, PhD; Masahiro Nishibori, MD, PhD

**Background and Purpose**—High mobility group box-1 (HMGB1) exhibits inflammatory cytokine-like activity in the extracellular space. We previously demonstrated that intravenous injection of anti-HMGB1 monoclonal antibody (mAb) remarkably ameliorated brain infarction induced by middle cerebral artery occlusion in rats. In the present study, we focused on the protective effects of the mAb on the marked translocation of HMGB1 in the brain, the disruption of the blood–brain barrier (BBB), and the resultant brain edema.

**Methods**—Middle cerebral artery occlusion in the rat was used as the ischemia model. Rats were treated with anti-HMGB1 mAb or control IgG intravenously. BBB permeability was measured by MRI. Ultrastructure of the BBB unit was observed by transmission electron microscope. The in vitro BBB system was used to study the direct effects of HMGB1 in BBB components.

**Results**—HMGB1 was time-dependently translocated and released from neurons in the ischemic rat brain. The mAb reduced the edematous area on T2-weighted MRI. Transmission electron microscope observation revealed that the mAb strongly inhibited astrocyte end feet swelling, the end feet detachment from the basement membrane, and the opening of the tight junction between endothelial cells. In the in vitro reconstituted BBB system, recombinant HMGB1 increased the permeability of the BBB with morphological changes in endothelial cells and pericytes, which were inhibited by the mAb. Moreover, the anti-HMGB1 mAb facilitated the clearance of serum HMGB1.

**Conclusions**—These results indicated that the anti-HMGB1 mAb could be an effective therapy for brain ischemia by inhibiting the development of brain edema through the protection of the BBB and the efficient clearance of circulating HMGB1. (*Stroke*. 2011;42:00-00.)

**Key Words:** blood–brain barrier ■ brain edema ■ electron microscopy ■ HMGB1 ■ MRI

Disruption of the blood–brain barrier (BBB) is a critical event in the formation of brain edema during the early phase of ischemic brain injury. BBB permeability can be increased by several factors, including cytokines, vascular endothelial growth factor, and nitric oxide.<sup>1,2</sup> Among these factors, cytokines have been widely described as vital players such as interleukin-1 $\beta$  and tumor necrosis factor- $\alpha$ .<sup>3,4</sup> High mobility group box-1 (HMGB1) is a ubiquitous and abundant nonhistone DNA-binding protein, which is newly defined as a cytokine that can be passively released from necrotic cells or positively released from immune activated cells under the stimulation of inflammatory signals, thus inducing inflammatory responses in sepsis, acute lung injury, and rheumatoid arthritis.<sup>5-7</sup> Recently, HMGB1 has received particular atten-

tion with respect to its pathological role in cerebral ischemia. In transient middle cerebral artery occlusion (MCAO) in mice and rats, HMGB1 was found to be translocated into the cytoplasmic compartment from nuclei.<sup>8-11</sup> High levels of serum HMGB1 were observed in patients with stroke compared with healthy control subjects.<sup>12</sup> This early release of HMGB1 into the extracellular space after ischemic injury may contribute to the initial stage of the inflammatory response in the ischemic penumbra.

We previously demonstrated that a neutralizing anti-HMGB1 monoclonal antibody (mAb) remarkably ameliorated brain infarction induced by a 2-hour MCAO in rats and was associated with significantly improved neurological deficits.<sup>9</sup> Although the disruption of the BBB was apparent by the extravasation of

Received August 6, 2010; final revision received November 14, 2010; accepted December 13, 2010.

From the Departments of Pharmacology (J.Z., H.K.T., K.L., H.W., R.L., M.N.), Neurosurgery (T.M., I.D.), Pathology (T.Y.), and Human Morphology (A.O.), Okayama University Graduate School of Medicine, Dentistry, and Pharmacological Sciences, Okayama, Japan; and the Department of Pharmacy (S.M.), Shujitsu University, Okayama, Japan.

The online-only Data Supplement is available at <http://stroke.ahajournals.org/cgi/content/full/STROKEAHA.110.598334/DC1>.

\*J.Z. and H.K.T. contributed equally to this work.

Correspondence to Masahiro Nishibori, MD, PhD, Department of Pharmacology, Okayama University Graduate School of Medicine, Dentistry and Pharmaceutical Sciences, Okayama 700-8558, Japan. E-mail: mbori@md.okayama-u.ac.jp

© 2011 American Heart Association, Inc.

Stroke is available at <http://stroke.ahajournals.org>

DOI: 10.1161/STROKEAHA.110.598334



Evans blue dye even at 3 hours after reperfusion in the control animals, the anti-HMGB1 mAb efficiently inhibited protein leakage and the activation of matrix metalloproteinase-9, which has been suggested to be an initial factor inducing endothelial tight junction (TJ) degradation in BBB disruption.<sup>13,14</sup> Therefore, we hypothesized that HMGB1 may contribute to BBB disruption during the acute phase of ischemia/reperfusion.

The present study was undertaken to further investigate the mechanism of the HMGB1-neutralizing mAb from the aspect of maintaining the BBB functionally and structurally. First, we analyzed the time course of HMGB1 translocation and release from brain cells into the cerebrospinal fluid and bloodstream. Second, we observed the changes in the structure of BBB using transmission electron microscopy and T2-weighted MRI. Third, we used the *in vitro* BBB system to demonstrate the direct effects of HMGB1 on the components of the BBB. The results strongly indicated that HMGB1 may induce morphological and functional changes in the BBB, whereas the anti-HMGB1 mAb prevented the increase of BBB permeability through the maintenance of its structure and facilitated the clearance of circulating HMGB1.

## Methods

### MCAO Surgical Procedure

All experimental procedures were conducted in accordance with the guidelines of Okayama University for animal experiments and approved by the university's committee on animal experimentation. Male Wistar rats (Charles River Laboratory Japan, Yokohama, Japan), weighing 250 to 300 g, were used for all experiments. MCAO was performed as previously described.<sup>9</sup> Briefly, the rats were anesthetized with 2% halothane in a mixture of 50% N<sub>2</sub>O and 50% O<sub>2</sub>. An 18-mm-long strand of 4/0 nylon thread coated with silicone was inserted into the right internal carotid artery to occlude the origin of the right middle cerebral artery. The thermocouple needle probe was inserted into temporal muscle to maintain the temperature at 37.0±0.1°C with a heating lamp during surgery. Only the rats that showed paralysis of the contralateral limbs after recovery from anesthesia were used for further experiments. Reperfusion was performed at 2 hours after MCAO. As shown in Supplemental Table 1 (<http://stroke.ahajournals.org>), basic physiological parameters, including blood gases, pH, hemoglobin, and glucose, were monitored. The rats were randomly assigned into 2 groups after MCAO operation, and an anti-HMGB1 mAb (#10-22, IgG<sub>2a</sub> subclass, 200 μg/rat) or class-matched control mAb (anti-Keyhole Limpet hemocyanin) was administered intravenously immediately and at 6 hours after reperfusion. All quantitative evaluation of animals was performed by investigators blinded to the treatment.

### Immunohistochemistry Staining

Paraffin-embedded brain sections were stained using a mouse anti-HMGB1 mAb (R&D Systems, Inc, Minneapolis, MN) or a rabbit anti-HMGB1 Ab (Abcam plc, Cambridge, UK). For double immunostaining, the sections were incubated with the mouse anti-HMGB1 mAb (R&D Systems, Inc) in combination with anti-microtubule-associated protein 2 Ab (Santa Cruz Biotechnology, Inc, Santa Cruz, CA), anti-glial fibrillary acidic protein Ab (Abcam plc), or anti-ionized calcium-binding adapter molecule 1 Ab (Wako, Inc, Osaka, Japan). For aquaporin 4 (AQP4) staining, a mouse anti-AQP4 mAb (Abcam plc) was incubated with frozen sections of rat brains as the primary antibody. See details in the Supplemental Methods (<http://stroke.ahajournals.org>).

### Enzyme-Linked Immunosorbent Assay of HMGB1

For HMGB1 determination in serum samples, blood samples (1 mL) were collected through the inferior vena cava under deep anesthesia using an intraperitoneal injection of sodium pentobarbital (50 mg/kg)

followed by centrifugation at 1500 g for 10 minutes. The supernatants were removed to clean Eppendorf tubes and stored at -20°C before use. Cerebrospinal fluid samples were collected from the cistern magna according to the previously reported method.<sup>15</sup> Samples contaminated by blood were excluded. HMGB1 was determined using an HMGB1 enzyme-linked immunosorbent assay kit (Shino-Test Co, Sagamihara, Japan) according to the manufacturer's protocol.

### Brain Water Content Measurement

Ten rats were allocated to 3 groups: the sham group (n=4), control mAb-injected group (n=8), and anti-HMGB1 mAb-injected group (n=9). All animals except the intact group were subjected to surgery for MCAO. Three hours after reperfusion, the animals were anesthetized deeply with an intraperitoneal injection of sodium pentobarbital (50 mg/kg). The brains were rapidly removed and dissected into 4 regions: the hippocampus, striatum, hypothalamus, and cerebral cortex in each hemisphere. After weighing, the tissues were dried at 80°C for 8 hours. The water content in each region was calculated according to the following equation: % water content=100×(wet weight-dry weight)/wet weight.

### MRI Examination

Rat brain water changes were examined in a 3.0-T horizontal-bore magnet (GE Signa EXCITE 3.0 T; GE Healthcare, Buckinghamshire, UK) at 3, 6, 12, and 24 hours after reperfusion (n=4 per group). MRI parameters were set with TR/TE=5000/15.18 ms, thickness/gap=2/0.2 mm, field of view=100 mm×100 mm, matrix=480×480, number of excitations=1.5. The body temperature was maintained at 37°C by a heating fan. After the optimal adjustment of contrast, hemisphere intensity was examined using National Institutes of Health image J 1.42q software (National Institutes of Health, Bethesda, MD) using the operation "mean gray value." The intensity percentage of the ipsilateral hemisphere against the contralateral hemisphere was calculated, and statistical analysis was performed. During MRI, a series of 4-slice data were obtained.

### Transmission Electron Microscopic Examination

Three hours after reperfusion, MCAO rats were anesthetized with an intraperitoneal injection of sodium pentobarbital (50 mg/kg) and perfused through the left ventricle with 50 mL of saline followed by 100 mL of 4% paraformaldehyde and 2.5% glutaraldehyde in 0.1 mol/L cacodylic acid buffer (pH 7.3). The fixed brain was dehydrated through an ethanol series embedded in epoxy resin and cut into ultrathin sections. The sections were mounted on copper grids, stained in uranyl acetate and citric acid lead, and then observed under a transmission electron microscope (H-7100; Hitachi Ltd, Tokyo, Japan) equipped in the central laboratory of Okayama University. To quantify the astrocyte end feet swelling, National Institutes of Health image J 1.42q software was used to calculate the ratio of the total swollen astrocyte end feet surrounding against the area of the corresponding capillary lumen. Eight rats were analyzed for each group treated with control Ab or anti-HMGB1 mAb. Seven capillaries in each area were evaluated.

### In Vitro BBB Permeability Assay

An *in vitro* BBB kit (RBE-12; PharmaCo-Cell Co Ltd, Sakamoto, Japan) composed of rat brain vascular endothelial cells, pericytes, and astrocytes was used to assess the effects of recombinant human HMGB1 (hHMGB1) and the mAb to the BBB unit according to the instructions of the manufacturer.<sup>16</sup> The endothelial cells were cultured on the bottom of the polyester membrane of the insert well. The pericytes were present below the membrane of the insert well. The astrocytes were cultured on the bottom of the lower chamber. Endotoxin-free rHMGB1 (see details in Supplemental Methods) alone or together with the anti-HMGB1 mAb was added into the lower chamber, which is supposed to be the brain side. Transendothelial electric resistance and leakage of the Evans blue-albumin complex were measured thereafter. F-actin was stained to observe the morphological changes of endothelial cells and pericytes. See detail in Supplemental Methods.



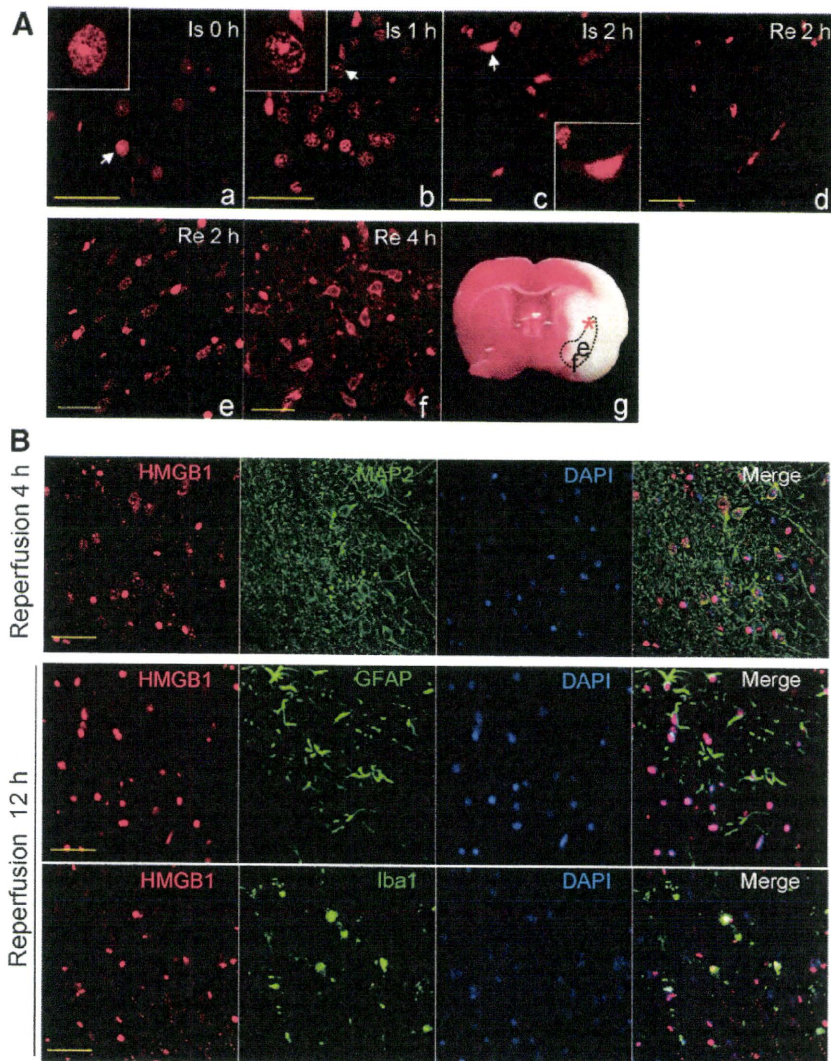


**Figure 1.** Time-dependent translocation of high mobility group box-1 (HMGB1) in neurons of ischemic rat brain. The rat brains were fixed before, during ischemia, and after reperfusion at different time points. **A**, In the normal rat brain (a), HMGB1 localized solely in cell nuclei with condensed staining in nucleoli. One hour after ischemia (b), HMGB1 was redistributed inside the nuclei forming a “lotus-root like structure” in the ischemic penumbra. Two hours after ischemia (c), the cells in the ischemic core of the striatum were reduced in size and HMGB1 was located in the nuclei and cytosol. **d**, Two hours after reperfusion, HMGB1 disappeared in neurons with big nuclei. The typical staining pattern of HMGB1 translocation was observed in the striatum of the ischemic rat brain fixed at 2 to 4 hours after reperfusion (e, f). **g**, 2-3-5-Triphenyl tetrazolium chloride staining of an ischemic rat brain 12 hours after reperfusion was shown to indicate the positions where the images (a–f) were obtained. The red asterisk in **g** indicated the places where the images (a–d) were obtained, which indicates the ischemic core in the striatum. The brain region surrounded by dashed line indicates the area where the typical translocation of HMGB1 was observed at a time point of 4 hours after reperfusion. **B**, HMGB1 translocated occurs in neurons but conserved in astrocytes and microglia cells even in the later phase of reperfusion. Sections were double stained with anti-HMGB1 antibody (Ab) and antimicrotubule-associated protein 2 (MAP2) Ab, antigitial fibrillary acidic protein (GFAP) Ab, or anti-ionized calcium-binding adaptor molecule 1 (Iba1) Ab. 4',6-Diamidino-2-phenylindole (blue) staining was used to show nuclear localization. All images were obtained from the cerebral cortex of the rat brain. Scale bars=50  $\mu$ m.

### In Vivo Brain Microdialysis

Rats were anesthetized using the same condition of the MCAO procedure and placed in a stereotaxic apparatus. Guide cannulae were implanted into the striatum (posterior, 0.25 mm; lateral, 4.0 mm from bregma; below the skull surface, 7.0 mm). Microdialysis probes (Eicom Co, Kyoto, Japan) were inserted through the guide cannulae. The probe was perfused with Ringer solution, and the microdialysis samples were collected. Glutamate in the samples was detected using a Shimadzu high-performance liquid chromatography system (Shimadzu Co, Kyoto, Japan) equipped with a C18 column (TSKgel ODS-100V; Tosoh Bioscience, Tokyo, Japan).<sup>17</sup> Before experiments, the in vitro recovery of each microdialysis probe was determined and all probes had 14% recovery at a flow rate of 4  $\mu$ L/min. See detail in Supplemental Methods.

### Statistical Analysis

Statistical significance was evaluated using 2-way analysis of variance followed by the Student *t* test. The statistical significance of the microdialysis experiments for glutamate was evaluated using 1-factor repeated-measures analysis of variance. The statistical significance of in vitro BBB experiments was evaluated using analysis of variance followed by Dunnett test. A probability value of <0.05 was considered to be significant.

## Results

### HMGB1 Translocation and Release

Immunohistochemical staining of HMGB1 showed that HMGB1 was localized solely in the nuclear compartment with the spotted staining of nucleoli throughout the brain from sham-operated rats (Figure 1Aa). After the onset of ischemia, HMGB1 was time-dependently translocated and released from the nucleus (Figure 1Ab–d). One hour after the onset of ischemia, HMGB1 changed its distribution inside the nucleus, forming a “lotus root-like structure,” suggesting the rapid reorganization of HMGB1 within the nucleus (Figure 1Ab). Two hours after the onset of ischemia, cells in the ischemic core had shrunk, to some extent, and HMGB1 was stained both in cytoplasm and the nucleus suggesting the translocation of HMGB1 (Figure 1Ac). Two hours after reperfusion, HMGB1 staining was partially lost in the ischemic core area (Figure 1Ad). The typical translocation of HMGB1 into the cytosolic compartment was evident in the ischemic core at 2 hours after reperfusion (Figure 1Ae) and peaked at 4 hours after reperfusion (Figure 1Af). Double immunostaining of HMGB1 and



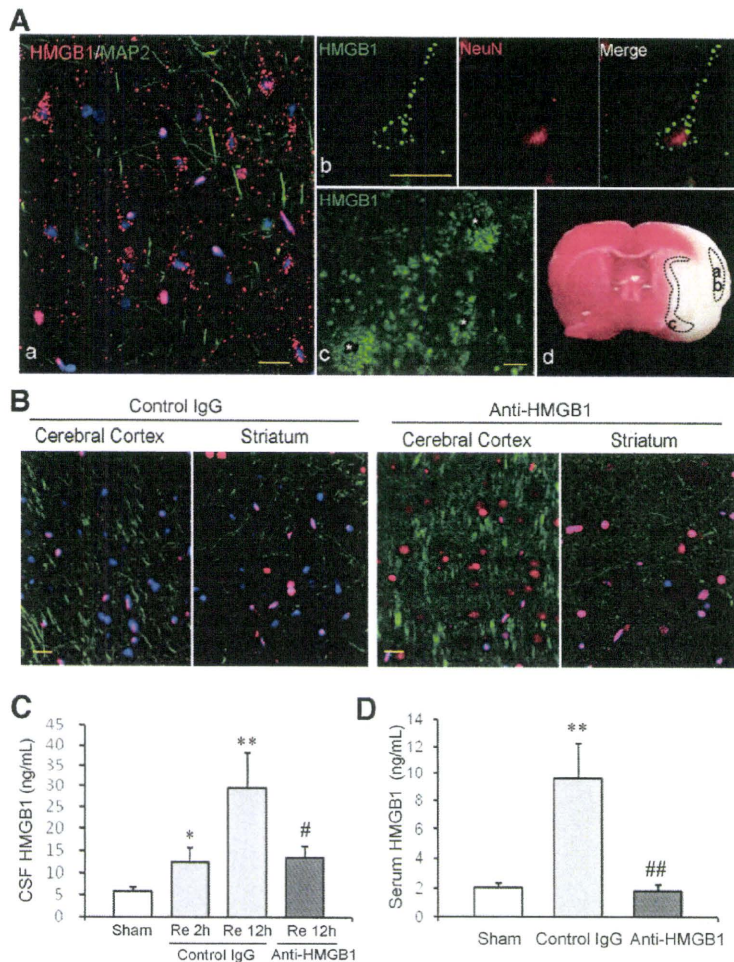


**Figure 2.** Translocation and release of high mobility group box-1 (HMGB1) from neurons and its inhibition by anti-HMGB1 monoclonal antibody (mAb). Coronal sections were prepared 12 hours after reperfusion. 4',6-Diamidino-2-phenylindole staining was performed to show the cell nuclei. **A**, HMGB1 was stained as a granule-like structure. **a**, HMGB1 (red) was stained as a granule-like structure aligning the neuron cell soma in the cerebral cortex. **b**, A representative cell stained both by anti-HMGB1 (green) and anti-NeuN Ab (red). **c**, HMGB1 staining (green) surrounding capillaries (asterisks) in the hypothalamus of the ischemia hemisphere. **d**, A 2-3-5-triphenyl tetrazolium chloride staining of an ischemic rat brain 12 hours after reperfusion was used to indicate the position where the corresponding images were obtained. The brain region surrounded by dashed line indicates the areas where the typical granule-like staining of HMGB1 were observed. Scale bars=20  $\mu$ m. **B**, Representative confocal images showing the inhibitory effects of the anti-HMGB1 mAb on HMGB1 translocation (red, HMGB1; green, microtubule-associated protein 2 [MAP2]). Scale bars=50  $\mu$ m. **C**, The HMGB1 levels in cerebrospinal fluid were determined using enzyme-linked immunosorbent assay (ELISA). The results are mean $\pm$ SEM of 10 (sham), 8 (2 hours in control IgG-treated group), 9 (12 hours in control IgG-treated group), and 9 (anti-HMGB1 mAb-treated group) rats. **D**, Serum levels of HMGB1 at 12 hours after reperfusion were determined using ELISA. The results are mean $\pm$ SEM of 8 (sham), 8 (control IgG-treated group), and 9 (anti-HMGB1 mAb-treated group) rats. \*\* $P$ <0.01 compared with sham control. # $P$ <0.05 and ## $P$ <0.01 compared with the group treated with control IgG (reperfusion).

microtubule-associated protein 2 revealed that the translocation mostly occurred in neurons (Figure 1B). In contrast, HMGB1 immunoreactivities in astrocytes and microglial cells were retained in nuclei even in the late phase of reperfusion (Figure 1B). Interestingly, in the ischemic core of the cerebral cortex, we observed a granule-like staining pattern of HMGB1 aligned on the neuronal cell soma, especially in the late phase of reperfusion (Figure 2Aa–b). In addition, the considerable number of small granule-like HMGB1 staining was observed surrounding the capillaries, especially in the hypothalamus of the ischemia hemisphere (Figure 2Ac). Figure 2B shows that at 12 hours after reperfusion, HMGB1 staining was almost completely lost in most of the cells in the ipsilateral side of the brain when compared with the rats treated with control IgG. In contrast, treatment with the anti-HMGB1 mAb inhibited the translocation and disappearance of HMGB1. Consistent with the results of immunostaining, we found that the HMGB1 level in the ischemic core area of the rat brain 12 hours after reperfusion significantly decreased to 40% and 44% in the striatum and the cerebral cortex, respectively, compared with the sham-operated rat (Supplemental Figure I).

Determination of HMGB1 using enzyme-linked immunosorbent assay showed that HMGB1 appeared in the cerebrospinal fluid as early as 2 hours after reperfusion and increased to 30 ng/mL 12 hours after reperfusion. Treatment

with anti-HMGB1 mAb significantly decreased the HMGB1 levels in cerebrospinal fluid (Figure 2C). Western blot analysis also supported that HMGB1 time-dependently increased in the cerebrospinal fluid (Supplemental Figure II). The increase of serum HMGB1 levels after ischemia was also observed in rats treated with control IgG, but the serum levels of HMGB1 were suppressed in anti-HMGB1 mAb-treated rats to the same level as in sham-operated rats (Figure 2D). To clarify whether the therapeutic anti-HMGB1 mAb affected the HMGB1 enzyme-linked immunosorbent assay results, we coincubated the anti-HMGB1 mAb with HMGB1 in rat brain homogenate or rHMGB1 and examined the incubated samples in the enzyme-linked immunosorbent assay plate. The results clearly show that the therapeutic mAb had no effects on the enzyme-linked immunosorbent assay (Supplemental Figure III). Meanwhile, in the anti-HMGB1 mAb-treated MCAO rats, levels of plasma 4-HNE adducts were also significantly reduced by 61% compared with that in control IgG-treated MCAO rats (Supplemental Figure IV).

#### Alleviation of Brain Edema

Brain edema is defined as an abnormal accumulation of fluid within the brain parenchyma, producing a volumetric enlargement of brain cells or tissue, which is one of the primary causes of clinical deterioration and a leading cause of death



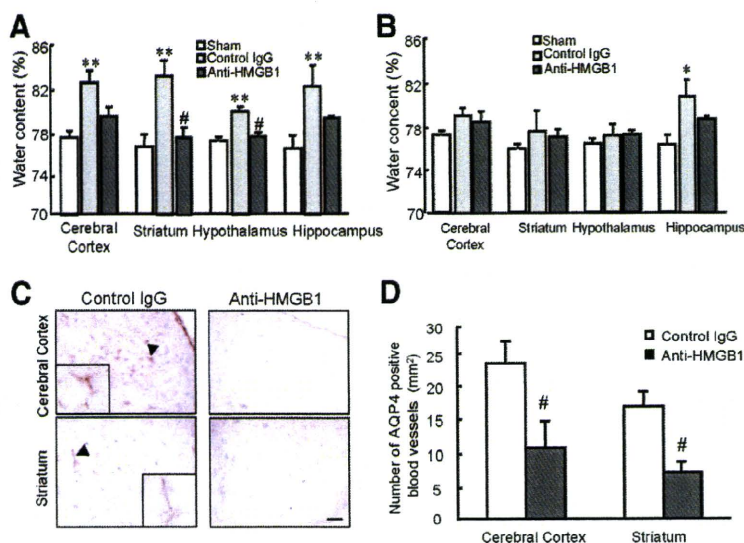


**Figure 3.** Brain water contents in rats treated with control IgG or anti-high mobility group box-1 (HMGB1) monoclonal antibody (mAb) at 3 hours after reperfusion. **A**, Ipsilateral hemisphere; **B**) contralateral hemisphere. The results are mean±SEM of the data from 4 (sham), 8 (control IgG-treated group), and 9 (anti-HMGB1 mAb-treated group) rats. \**P*<0.05 and \*\**P*<0.01 compared with the sham-operated group. #*P*<0.05 compared with control IgG group. **C**, Immunohistochemical staining of aquaporin 4 (AQP4) in the brain sections from 2-hour middle cerebral artery occlusion (MCAO) rats. The rats were treated with the anti-HMGB1 or control mAb immediately after reperfusion. The tissues were fixed by infusing formalin transcardially at 3 hours after reperfusion. Coronal frozen sections were stained with an anti-AQP4 mAb as described in "Methods." Insets represent the higher magnification picture of indicated structure by arrows. Scale bar=100 μm. **D**, Quantitative results of AQP4 staining by counting the AQP4-positive blood vessels. The results are mean±SEM of the data from 5 rats. #*P*<0.05 compared with the control IgG group.

after ischemia/reperfusion. In the sham group, the brain water content formed 76% to 78% of the total weight. Three hours after reperfusion, in the rats treated with control IgG, the brain water contents in the cerebral cortex, striatum, hypothalamus, and hippocampus of the ischemic hemisphere had significantly increased to 82.8%, 83.3%, 80.0%, and 82.3%, respectively. In contrast, the anti-HMGB1 mAb attenuated the increase in water content by 3.2%, 5.7%, 2.3%, and 2.85% in each region, respectively (Figure 3A). The hippocampal edema occurred not only in the ischemic side, but also in the nonischemic side that was also inhibited by treatment with the anti-HMGB1 mAb (Figure 3B).

AQP4 is a prominent biological marker to determine the permeability of brain capillaries in brain edema.<sup>18,19</sup> Figure 3C shows that in the MCAO rats (3 hours after reperfusion) treated with control IgG, the immunoreactivity of AQP4 in the cerebral cortex and striatum was significantly increased. It appears that AQP4 was strongly expressed in capillary vessels, probably on the astroglial membranes<sup>20</sup> that had direct contact with the lamina propria. The results of AQP4 immunohistochemistry were quantitatively determined by counting the AQP4-positive blood vessels (Figure 3D). The treatment with anti-HMGB1 mAb remarkably inhibited the expression of AQP4 both in the cerebral cortex and striatum.

**MRI Studies**

MRI is considered the most promising and noninvasive tool for recognizing brain edema formation in real time. T2-weighted MRI is frequently used to determine the presence or absence of edema, especially vasogenic edema induced by reperfusion.<sup>21</sup> Consistent with the data for brain edema determined by the water content, T2-weighted MRI clearly showed time-dependent changes in brain edema in the ischemic areas containing the striatum, cerebral cortex, and hippocampus in the control rats. The representative data from 5 rats are shown in Figure 4A. Three hours after reperfusion, striatal edema was evident in the control Ab group. At 6 hours after reperfusion, the edematous areas had expanded to the cerebral cortex. Treatment with the anti-HMGB1 mAb inhibited the increase in the intensity of the images in the ischemic

areas (Figure 4A). Figure 4B summarizes the quantitative analysis of MRI based on intensity analysis of the images in the ischemic hemisphere against those in the contralateral hemisphere. At 24 hours after reperfusion, the high intense T2 signal in the control rats may contain a necrotic area. Before Ab treatment, the physiological parameters such as the neurological scores and Rotorod test scores were not different

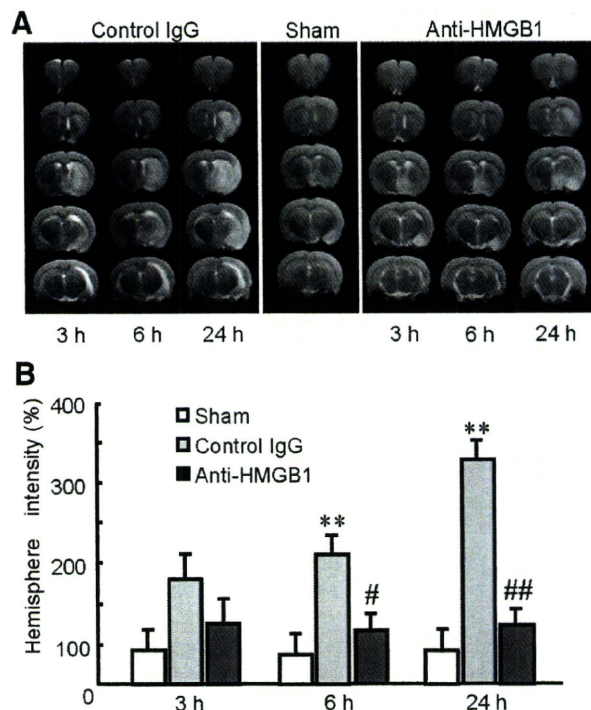


**Figure 4.** Serial T2-weighted MRI obtained from rats treated with control IgG or anti-high mobility group box-1 (HMGB1) monoclonal antibody (mAb). **A**, Representative MRI from rats in the control, anti-HMGB1, and sham groups. Time points indicate the intervals after reperfusion. **B**, Percentage of the intensity in the ipsilateral hemisphere against that in the contralateral hemisphere at various time points after reperfusion. The results are mean±SEM of 5 animals in each group. \**P*<0.05 and \*\**P*<0.01 compared with sham; #*P*<0.05 and ###*P*<0.01 compared with the control group.

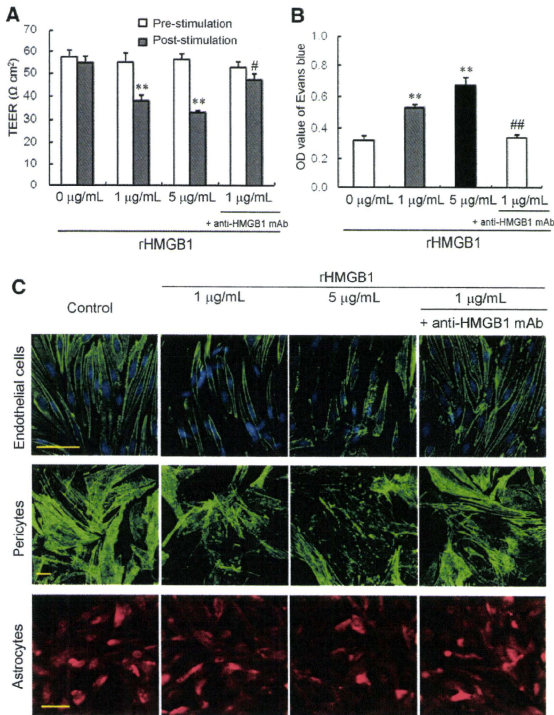


**Figure 5.** Effects of recombinant high mobility group box-1 (rHMGB1) on the permeability of rat reconstituted blood-brain barrier (BBB) *in vitro*. The rat-reconstituted BBB system composed of vascular endothelial cells, pericytes, and astrocytes was used for the experiments. **A**, Recombinant HMGB1 at 1 or 5 μg/mL was added to the brain side (lower chamber), and the incubation continued for 60 minutes. When the anti-HMGB1 monoclonal antibody (mAb) was added, the mAb at 2 μg/mL was preincubated with rHMGB1 for 30 minutes. Transendothelial electric resistance (TEER) was measured before and after rHMGB1 stimulation. The results are mean±SEM of 3 independent experiments. \*\**P*<0.01 compared with the corresponding value before stimulation. #*P*<0.05 compared with the value in the presence of rHMGB1 (1 μg/mL) alone. **B**, After the detection of TEER, Evans blue with albumin was added to the insert well and the incubation continued for 30 minutes. The transudated Evans blue dye into the lower chamber was determined. The results are mean±SEM of 3 independent experiments. \*\**P*<0.01 compared with the value in the absence of rHMGB1. ##*P*<0.01 compared with the value in the presence of rHMGB1 (1 μg/mL) alone. **C**, After 1 hour stimulation with rHMGB1, the cells were fixed with 4% paraformaldehyde for 30 minutes. Endothelial cells and pericytes were labeled with alexa-488-phalloidin and 4',6-diamidino-2-phenylindole and observed under confocal microscope. Astrocytes were observed by Evans blue fluorescence. Scale bars=50 μm.

between the anti-HMGB1 mAb and control IgG-treated groups (data not shown).

### In Vitro BBB Permeability Assay

Using an *in vitro* BBB system composed of rat brain vascular endothelial cells, pericytes, and astrocytes, the direct effects of rHMGB1 on the permeability of BBB were examined (Figure 5). The rHMGB1 generated from inset cells (free of lipopolysaccharide) was added into the brain side (lower chamber) at a concentration of 1 μg/mL and 5 μg/mL, and the incubation continued for a total of 60 minutes. The addition of rHMGB1 concentration-dependently decreased the transendothelial electric resistance, and mAb antagonized the reduction of transendothelial electric resistance induced by rHMGB1, whereas the transendothelial electric resistance levels before stimulation were the same among groups (Figure 5A). The stimulation with rHMGB1 concentration-dependently increased the permeability of the Evans blue-albumin complex. The mAb significantly inhibited the enhanced permeability of BBB indicated by Evans blue-albumin leakage (Figure 5B).

Consistent with the results of the dye leakage and the reduction of transendothelial electric resistance, the stimulation

with rHMGB1 induced the morphological changes in pericytes and endothelial cells. In pericytes, the F-actin staining reduced after the stimulation with rHMGB1 concentration-dependently. Also, the vascular endothelials seemed to shrink longitudinally, leading to the intercellular space formation. These morphological effects of rHMGB1 were antagonized by the addition of anti-HMGB1 mAb. In contrast, there was no difference in astrocyte shape among groups examined (Figure 5C).

### Electron Microscopic Observation of the BBB

Images from transmission electron microscopy clearly identified the BBB unit composed of endothelial cells, basal lamina, pericytes, and astrocyte end feet. Figure 6A shows representative images of the BBB unit in the striatum. In the control IgG rat brains fixed at 3 hours after reperfusion, it is evident that the astrocyte end feet were swollen to various extents in the ischemic regions (Figure 6Aa–b). In many cases, the intracellular organelles were absent or scarce in such swollen astrocyte end feet labeled by asterisks in Figure 6Aa. In addition to the enlargement of astrocyte end feet, the detachment of the end feet plasma membrane from the basal lamina was observed (arrows